Chemical Engineering Research and Design 204 (2024) 97–111

Contents lists available at ScienceDirect

Chemical Engineering Research and Design

journal homepage: www.elsevier.com/locate/cherd

Enviro-economic investigation of Novel heat-integrated configurations for pressure swing distillation

Abbas Gholami [a], Norollah Kasiri [a,*], Amirhossein Khalili-Garakani [b], Juan Gabriel Segovia-Hernández [c]

[a] Computer Aided Process Engineering (CAPE) Laboratory, School of Chemical Petroleum and Gas Engineering, Iran University of Science & Technology (IUST), Tehran 168461-3114, Iran
[b] Chemistry & Process Engineering Department, Niroo Research Institute (NRI), Tehran 1468613113, Iran
[c] Universidad de Guanajuato, Facultad de Química, Noria Alta s/n, Guanajuato 365050, Mexico

ARTICLE INFO

Keywords:
Pressure swing distillation
Energy efficiency
Internal heat integration
External heat integration
Heat Integration

ABSTRACT

Pressure Swing Distillation is a widely adopted solution for the separation of pressure-sensitive azeotropic mixtures in various chemical industries. While this method yields high-purity products, it comes with inherent challenges such as elevated operating costs and energy consumption. However, the temperature differential between the two columns involved presents a compelling opportunity for heat integration. In this study, 18 distinct heat integration scenarios were systematically evaluated using a process simulation software to identify the optimal column configuration for minimizing the Total Annualized Cost. These scenarios span five categories: the Conventional Method, Partial Heat Integration, Full Heat Integration, Internal Heat Integration Distillation Column, and External Heat Integration Distillation Column. The Vapor Recompression Column and Divided Wall Column schemes were applied to each method. Genetic Algorithm served as the optimization tool to determine the best arrangement with TAC as the objective function. Additionally, the environmental impact, assessed through CO_2 emissions, was considered. Results indicate that the most economically and environmentally friendly solution is the I-HIDiC with divided wall columns, incorporating VRC systems in both columns. This approach offers a remarkable 66.5% cost savings and a substantial 96.3% reduction in CO_2 emissions.

1. Introduction

Distillation is the most common industrial process for separation, which despite its simplicity, has high energy consumption and low thermodynamic efficiency (η). Azeotropes cannot be separated through conventional distillation (Huang et al., 2010; Lü et al., 2018). Thus different methods are used to separate azeotropes, including extractive distillation (Xu et al., 2022; Zhang et al., 2021), azeotropic distillation (Li et al., 2022; Qi et al., 2020), and Pressure Swing Distillation (PSD) (Zhu et al., 2021; Shi et al., 2020). The PSD process is one of the prime methods used for pressure-sensitive mixture separation (Zhang et al., 2020). If the azeotrope molar point changes at least 5% by applying a pressure change of 10 bar, PSD is used for separation (Ferchichi et al., 2022). Minimum and maximum boiling point azeotropes can be separated using the PSD process involving two columns at two different pressures. One product is taken from each column. Products are taken from the bottom of the column at minimum boiling point azeotrope, while at maximum boiling point azeotrope, products are taken from the top. Another product composition is close to the azeotropic point (Ferchichi et al., 2022; Xia et al., 2017; Wang et al., 2019).

The main advantage of PSD compared to other methods is obtaining products with high purity due to the absence of the third component (solvent) (Wang et al., 2016; Li et al., 2019a). PSD process has the simplicity of implementation and the possibility of thermal integration due to an appropriate temperature difference between the two columns. Unlike other methods, it has no costs related to the solvent and makeup streams. While this method has many advantages, it also has relatively high operating and capital costs due to using a column at high pressure (Zhu et al., 2015; Liang et al., 2017).

Acetonitrile (ACN), or Methyl cyanide, is an organic solvent widely used in the agrochemical, organic synthetic, petrochemical, and pharmaceutical industries (McConvey et al., 2012; Zhang et al., 2011). Purifying butadiene and fatty acids is its primary use (Qi et al., 2020; Li et al., 2019a). It is produced as a byproduct of the acrylonitrile production process (Sazonova and Raeva, 2015; Rezaie et al., 2020). ACN

* Corresponding author.
E-mail address: capepub@iust.ac.ir (N. Kasiri).

https://doi.org/10.1016/j.cherd.2024.02.033
Received 3 December 2023; Received in revised form 4 February 2024; Accepted 15 February 2024
Available online 18 February 2024

Nomenclature

PSD	Pressure Swing Distillation
TAC	Total Annualized Cost
PHI	Partial Heat Integration
FHI	Full Heat Integration
HIDiC	Heat Integration Distillation Column
IHIDiC	Internal Heat Integration Distillation Column
EHIDiC	External Heat Integration Distillation Column
VRC	Vapor Recompression Column
DWC	Divided Wall Column
GA	Genetic Algorithm
ACN	Acetonitrile
HPC	High-Pressure Column
LPC	Low-Pressure Column
COP	Coefficient Of Performance
η	Thermodynamic efficiency
COPS	Coefficient Of Performance Simplified
Q_{CON}^{HPC}	Condenser duty of high-pressure column
Q_{REB}^{LPC}	Reboiler duty of low-pressure column
M$	Million dollar
F1	Low-pressure column feed
F2	High-pressure column feed
R1	Reboiler of low-pressure column
R2	Reboiler of the high-pressure column
C1	Condenser of the low-pressure column
C2	Condenser of the high-pressure column.
B1	Boil up of low-pressure column
B2	Boil up of high-pressure column
RS	Recycle Stream
RF1	Reflux of low-pressure column
RF2	Reflux of high-pressure column

and water cannot be separated by conventional distillation because of the formation of a minimum boiling point azeotrope (Qi et al., 2020). Water may be separated from ACN by extractive distillation (Qi et al., 2020; Sazonova and Raeva, 2015), azeotropic distillation (Qi et al., 2020), and PSD (Li et al., 2019a).

Qi et al. compared azeotropic and extractive distillation with PSD configuration for water and ACN. The azeotropic distillation using benzene as the entrainer and ethylene glycol were used in the extractive distillation method. Thermal integration was carried out for all three methods, and different configurations were analyzed using economic and environmental indicators. This investigation found that azeotropic distillation is a more attractive option than other methods from an economic and environmental viewpoint (Qi et al., 2020). In 2019 another research was conducted by Li et al. showing Full Heat Integration (FHI) reduces the Total Annualized Cost (TAC) by 32.39% compared to the conventional configuration (Li et al., 2019a).

The Vapor Recompression Column (VRC) technique is one of the important methods to increase the efficiency of the distillation process. In this technique, a compressor is used to remove the reboiler from the process by increasing the pressure. The idea of Heat Integration Distillation Column (HIDiC) is also one of the techniques that use a compressor to create a temperature difference in two sections of the distillation tower and then uses the existing temperature difference in order to reduce the amount of thermal energy consumption (Kiss and Smith, 2020). Another method used to reduce energy consumption in distillation column processes is the use of the Divided Wall Column (DWC) technique. The DWC is a column with a middle wall and is designed to separate mixtures of three or more components into high-purity products. A DWC requires much less energy consumption, capital cost, and space compared to conventional columns (Dejanović et al., 2010). Of course, other methods such as absorption heat pump, compression-resorption heat pump, thermo acoustic heat pump, bottom flashing, etc. are used to intensify the distillation process (Kiss and Smith, 2020; Kazemi et al., 2018).

Due to the temperature difference between the two columns, heat integration reduced energy consumption in the PSD process (Huang et al., 2008; Shan et al., 2021). Implementation of thermal integration for PSD has two ways. One is the possibility of heat transfer between the condenser of the High-Pressure Column (HPC) and the reboiler of the Low-Pressure Column (LPC), which reduces energy consumption. This method includes Full Heat Integration (FHI) and Partial Heat Integration (PHI) configuration. The second type includes heat transfer between the rectifying section of HPC and the stripping section of LPC (Huang et al., 2008; Shan et al., 2021).

Mariem et al. studied the separation of water and ethylenediamine azeotrope. A variety of configurations are used in this study to separate azeotropes. Using PHI is a more attractive option than FHI, from both economic and environmental viewpoint (Ferchichi et al., 2022). Li et al. investigated the azeotrope of ACN and water. Conventional configurations and FHI were simulated and optimized. The results showed that thermal integration has many advantages (Li et al., 2019a).

To reduce costs, heat pump technology has been applied as one of the most popular methods of thermal coupling in distillation processes (Ferchichi et al., 2022; You et al., 2019). In addition to reducing energy consumption, this method also increases η (Huang et al., 2008; Shan et al., 2021). The fundamental thermodynamic principle of operation is to use work to produce temperature differences that permit heat transfer (Luyben, 2018). Li et al. used the heat pump in a PSD process to separate ethanol from ACN and found that the use of heat pump on both columns, simultaneously or separately, was possible (Li et al., 2019b). Ferchichi et al. investigated the feasibility of using the heat pump for water and ethylamine separation. Using a heat pump in the LPC led to a 16.5% reduction in TAC compared to the HPC (Ferchichi et al., 2022).

One of the challenges in energy saving is internal and external heat integration (Huang et al., 2008; Shan et al., 2021). Several studies have been conducted to develop a systematic method of thermal integration both internally and externally (Maddu and Malik, 2011; Gadalla et al., 2007; Shahandeh et al., 2015). In one of these studies, Amiya K. Jana examined and compared all methods of thermal integration in distillation columns, including Diabatic, Fractionating heat exchangers, DWC, Petlyuk, Internal Heat Integration Distillation Column (IHIDiC), and External Heat Integration Distillation Column (EHIDiC) (Jana, 2010, 2016). Maddy et al. investigated internal heat integration and presented an 8-step method for its simulation and optimization. It was shown that IHIDiC has excellent performance for separating a binary mixture. However, this method has no favorable results for multi-component streams (Maddu and Malik, 2011). Shahandeh et al. investigated different internal and external thermal integration layouts. This research presents appropriate algorithms for economic optimization based on TAC objective functions for IHIDiC and EHIDiC and evaluates various cases (Shahandeh et al., 2015, 2014). In 2019, Khalili et al. used the concept of external thermal integration in ternary distillation towers to separate benzene, toluene, xylene, and normal alkanes. This research investigated various locations for the heat exchanger, and the best place was selected, which led to a 22.6% reduction in annual costs. The use of external thermal integration by the middle wall was determined to be the most efficient arrangement, which led to a decrease of 39% in TAC (Khalili et al., 2020).

A. Gadalla has presented a systematic design methodology for IHIDiC. An IHIDiC design hierarchy based on two phases of design is developed. The two phases of design are thermodynamics and hydraulics. Temperature profiles are an important component of heat integration, whereas hydraulic calculations are necessary for quantifying the efficiency of a column design in place of heat panels (Gadalla, 2009). Suphanit presented a procedure for IHIDiC design. To create this system, he introduced two methods: uniform heat transfer area and constant heat transfer load. He used the total amount of heat rejected from the rectifying section and the total amount of heat required in the stripping section for determining the desired specifications, such as heat distribution profile and column parameters. In the first step, heat transfer per tray was found, and in the next section, heat panel area per tray was determined. Under uniform heat transfer area mode, heat transferred from each tray to the corresponding tray is directly related to the temperature difference between the two trays and is calculated from Eq.1, in which Q_T is the total heat that can be transferred between the two sections, and ΔT_i shows the temperature difference between the two trays. The possibility of achieving large and impractical areas is the weakness of this method.

$$Q_i = \Delta T_i \quad \frac{Q_T}{\sum_{i=1}^{n} \Delta T_i} \tag{1}$$

For the uniform heat load approach, dividing the total heat by the number of trays is enough.

$$Q_i = \frac{Q_T}{n} \tag{2}$$

The obtained values have been placed in the simulator, and various factors' effects have been evaluated and investigated (Suphanit, 2010).

A. Kiss et al. investigated HIDiC in 2014. In this research, rectifying section of a distillation column operating at a higher pressure becomes the heat source, while the stripping part of the column acts as the heat sink. Various layouts for the IHIDiC implementation were investigated and evaluated. Inter-coupled distillation columns, Concentric distillation columns, Distillation columns with partition walls, Concentric columns with heat panels, and Shell and tube heat-exchanger columns are examples of the proposed methods for using the concept of IHIDiC (Kiss and Olujić, 2014).

Recently, a lot of research have been done by researchers to reduce energy consumption in the PSD process. Zhang et al. carried out a research on the implementation of PSD on the separation of benzene and isobutanol using HIDiC and VRC to reduce energy consumption. Using the idea of VRC and HIDiC has led to a reduction of 74.26% and 69.74% in energy consumption, respectively. Also, the use of VRC and HIDiC ideas has led to a 66.61% and 57.48% reduction in CO_2 emission, respectively (Zhang et al., 2022). Zhai et al. used the ideas of VRC and HIDiC in PSD to reduce energy consumption in the separation of isopropanol from wastewater. According to the results of this research, the implementation of these two ideas on PSD has many advantages both in terms of the TAC and from the environmental point of view (Zhai et al., 2023). Many other researchers have also used the ideas of VRC, and HIDiC to reduce energy consumption in PSD, but the main point is to combine and apply these ideas together, which has not been paid attention to.

The present research used the PSD process to separate water-ACN pressure-sensitive azeotropes. The temperature difference between the two columns as a driving force for heat transfer helped reduce operating costs and TAC significantly. For this process, eighteen configurations were presented. These configurations are simulated in the simulation environment with the genetic algorithm (GA) used in MATLAB for economic optimization. Carbon dioxide emission was chosen as an environmental friendliness indicator, with η as another indicator. The coefficient of performance (COP) was used as an indicator to evaluate the performance of heat pumps. The innovation of this research was the simultaneous use of the heat pump idea and internal or external thermal integration to implement PSD, which led to the creation of several new layouts. The strategic idea in this research is to achieve a set of logical layouts for the PSD process and to choose a process that is economically superior to other layouts. So far, no comprehensive research has been done on the subject. It should be noted that internal and external thermal integration has never been used for the PSD process despite the temperature difference between the two columns. Using these ideas and combining them with VRC has led to the emergence of new arrangements. Of course, the final and main goal is to create a space to investigate all azeotropic separation methods such as PSD, extractive distillation, and azeotropic distillation, so that for a specific case, the best and most economical arrangement can be chosen for industrialization.

This research introduces six new arrangements in PSD configurations through the following procedure.

- Initially these structures are proposed using internal heat integration with two concentric columns.
- Then the VRC concept and internal heat integration are applied with two concentric columns, resulting in new arrangements.
- The introduction of configurations then utilizes internal heat integration through the DWC for PSD.
- The VRC concept and internal heat integration with the middle wall column lead to new arrangements.
- Configurations based on external heat integration for PSD are introduced.
- Finally an approach incorporates the idea of VRC and EHIDiC to achieve new arrangements.

The incorporation of VRC and thermal integration strategies not only significantly reduces annual costs but also leads to a substantial decrease in carbon dioxide emissions, accompanied by a notable increase in η. These results provide the foundations for selecting the most optimal economic-environmental configuration.

2. Method

2.1. Feasibility study

The PSD process may only be used when the azeotropic point is pressure-sensitive. Analyzing equilibrium data is necessary to determine the degree of sensitivity. To describe the vapor-liquid equilibrium conditions, the NRTL model is applied. The EC Carlson method was used to select the fluid package (Carlson, 1996). Fig. 1-A shows the mole fraction and azeotropic point temperature plot as a function of pressure. Fig1-B shows XY diagram for ACN and water mixture in atmospheric pressure. According to Fig. 1-A, it is clear that this azeotrope is pressure-sensitive. Therefore, the PSD process can be an appropriate method for separating the ACN-water azeotrope. In Fig. 1-C, TXY graphs are drawn at two pressures of 1 and 9.63 bar. In this diagram, the possibility of separating water and ACN is clearly defined.

2.2. Simulation

The simulation of all arrangements except for those based on internal thermal integration has been carried out in a process simulation environment. Normally modeling of layouts based on internal thermal integration has two stages. In order to simulate and determine the transferred heat, the heat loss section in the distillation columns was used and coding was done to perform economic calculations. It should be noted that simulation, modeling, and optimization have been done simultaneously, which leads to the complexity of the calculations. A two-step procedure has been used to simulate systems based on thermal integration. Initially, the process is simulated and with the first optimization, the values related to the optimization variables (the number of trays per tower, inlet tray, reflux ratio, etc.) are determined. Then the optimal values are placed in the simulator, and the number of thermal

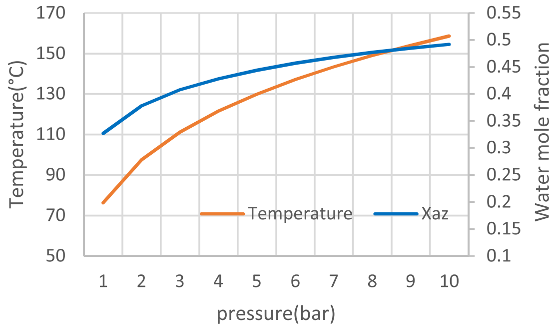

A: The azeotrope's temperature and composition as a function of pressure.

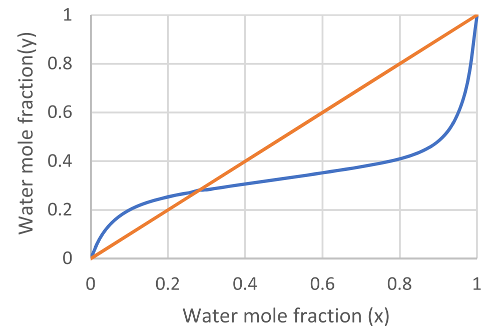

B: XY diagram for WATER/ACN at atmospheric pressure

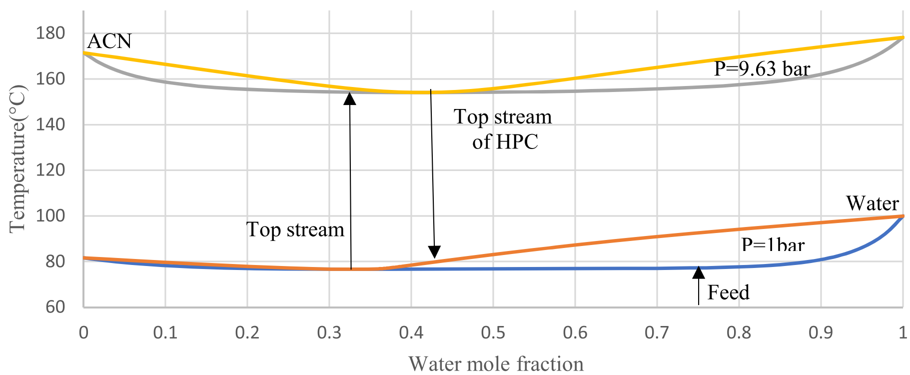

C: TXY diagram for WATER/ACN at P=1bar, P=9.63bar

Fig. 1. : Three vapor-liquid diagram of ACN-Water.

panels is determined using the optimization of the presented model. The NRTL thermodynamic package has been used to simulate this process. The binary coefficients related to this equation are shown in Table1. More information on how simulations are carried out is provided in Appendix A.

2.3. Optimization

The objective function is to optimize the TAC. Appendix A includes the formulas used to estimate costs (Zhu et al., 2015), (Li et al., 2019b). Configurations are optimized in MATLAB 2018 using GA. In the GA optimization, the number of populations in each generation is 100, the number of generations is 300, and the Crossover Fraction is 0.8. The annual operational time is 8150 hrs., with a yearly interest rate of 10% and a ten-year payback period. As a constraint of optimization, the purity of the products is set at more than 99.9 mol percent. To determine the column's design parameters and sieve trays, the "Tray sizing" function was used. For TAC calculations, 0.568 kW/ (m^2.K) and 0.852 kW/(m^2.K) were used for the reboiler and condenser, respectively. According to the CEPCI,[1] M&S is 1773.4.

Table 1
NRTL binary parameters for water-ACN at APV120 VLE-IG source and temperature between(60–94.9) °C.

Component i=Water	A_{ij}	A_{ji}	B_{ij}
Component j=ACN	1.0567	-0.1164	283.4087
	B_{ji}	**C_{ij}**	**D_{ij}**
	256.4588	0.3	0

[1] Chemical Engineering Plant Cost Index

2.4. Environmental analysis

The amount of carbon dioxide emission is a crucial indicator for the process's environmental assessments. The release of carbon dioxide in processes occurs due to various reasons, the most important of which is the production of steam in reboilers or furnaces, as well as the power consumption of compressors. The following equation calculates carbon dioxide emission from reboilers' steam production.

$$[CO2]_{emission} = Q_{fuel} \cdot Fuel_{factor} \tag{3}$$

$$Fuel_{factor} = \left(\frac{\alpha}{NHV}\right) \cdot \left(\frac{(C\%)}{100}\right) \tag{4}$$

Q_{fuel} is the amount of power obtained from burning fuel, and α equals the ratio of carbon dioxide's molecular mass to carbon's molecular mass (3.67). The NHV (kj/kg) indicates the net heating value of the fuel, which is 39771 kj/kg for heavy fuel oil and 51600 kj/kg for natural gas. The C% of the fuel is also equal to the carbon content, which for heavy fuel oil equals 86.5, and for natural gas is 75.4.

$$Q_{Fuel} = \left(\frac{Q_{reb}}{\lambda_{proc}}\right) \cdot (h_{proc} - 419) \cdot \left(\frac{T_{ftb} - T_0}{T_{ftb} - T_{stack}}\right) \tag{5}$$

λ_{proc} (kJ/kg) shows the latent heat of vaporization of the steam entering the system, and h_{proc} (kJ/kg) is related to the enthalpy of the steam entering the system. T_{ftb} is the theoretical temperature of the flame at 1800 °C, and T_{stack} represents the chimney temperature at 160 °C. T_0 is the ambient temperature, and the number 419 is related to the enthalpy of the boiler water at 100°C. Q_{reb} is the required heat in the reboiler in kilowatts. This research assumes that there is enough excess air during combustion to prevent improper discharge and the formation of carbon monoxide. The required energy is supplied by heavy fuel oil. The amount of carbon dioxide emission in compressors equals 51.5 kg of carbon dioxide per gigajoule of energy consumed (You et al., 2016; Wang et al., 2020).

2.5. Thermodynamic efficiency

The η is the index for evaluating the process efficiency. This index shows the efficiency of energy consumption in the system and is calculated by Eqs. 6–9.

$$\eta = \frac{W_{\min}}{LW + W_{\min}} \quad (6)$$

$$W_{min} = \sum_{out} nb - \sum_{in} nb \quad (7)$$

$$b = h - T_0 s \quad (8)$$

$$LW = \sum_{in}\left[nb + Q_R\left(1 - \frac{T_0}{T_S}\right) + W_{comp}\right] - \sum_{out}\left[nb + Q_C\left(1 - \frac{T_0}{T_S}\right) + W_{comp}\right] \quad (9)$$

W_{min} (kj/h) represents the minimum separation work (ideal work of the process), and LW means the lost work (kJ/h) with h (kj/kmol) and s (kj/kmol•K) describing the enthalpy and entropy at the inlet and outlet streams, respectively. The exergy is b (kj/kmol), the molar flow rate is n (kmol/h), T_0 is the environmental temperature (K), and T_s is the heat source or heat trap temperature. Q_R and Q_C represent reboiler and condenser duties, and compressor work is W_{comp} (kJ/h) (Wang et al., 2020; Mao et al., 2020).

2.6. Heat pump performance

The performance coefficient is an indicator for evaluating the operation of heat pumps. This value represents the ratio of heat the hot source receives to the amount of work consumed by the compressor (Zhang et al., 2020). Eqs. 10 and 11 are used to evaluate the performance of heat pumps.

$$COP = \frac{Q_H}{W} \quad (10)$$

The simple performance coefficient indicates whether the heat pump idea is suitable for distillation or not.

$$COPS = \frac{Q_R}{W} = \frac{T_C}{T_R - T_C} \quad (11)$$

Q_R is the reboiler duty of the column, and W represents the work of the compressor. T_R and T_C are reboiler and condenser temperatures, respectively (K). If *COPS* is greater than 10, using a heat pump has many advantages. When *COPS* is between 5 and 10, more detail is required to determine whether a heat pump is suitable or not. When *COPS* is less than 5, heat pumps are not recommended (You et al., 2016).

3. Configurations

3.1. Conventional PSD

Feed specifications are shown in Table2. The NRTL activity coefficient model is used to estimate the thermodynamic properties. The pressure of the first column is 1 bar due to vacuum problems, costs, ease of operation, and controllability. The conventional PSD process is illustrated in Fig. 2. The number of trays, the inlet tray, the two-column reflux ratio, the pressure of the HPC, the recycle stream flow rate, and the recycle stream inlet tray in the first column are optimization variables. The bottom products flow rates in both columns are fixed. The two tower pressures are 1 and 9.63 bars respectively. The conventional layout is one of the four basic layouts on which other ideas are applied to create a new sequence.

Table 2
Feed specifications.

Pressure(bar)	1	
Temperature(°C)	25	
Component molar flowrate (kmole/hr)	H_2O	75
	C_2H_3N	25

The range of optimization variables has a very significant effect on reaching the optimal point. To ensure that all states and conditions are considered, the range of variables is considered wide. Table3 shows the optimization variables and their upper and lower bounds. It should be noted that the variable related to the inlet tray should not be greater than the number of trays and that this rule has been observed throughout the optimization coding.

For optimization, the simulator is linked to Matlab. In this process, the Matlab and the simulation files must be in the same place. After calling and opening the simulation files in MATLAB, the settings related to the GA will be determined. At this stage, the number of variables, the upper and lower limits of the variables, the number of populations, the number of generations, the cross-over factor and mutation factor, and the restrictions related to the end of the optimization should be specified. In the next step, the initial population is created using the given upper and lower bounds and the rand function in Matlab. In the next step, the constraints related to the variables are defined. For example, it should be noted that the feed input estimated by the GA should not exceed the total number of trays estimated by this algorithm. In the final step, the mentioned settings and economic evaluation files are executed simultaneously and finally, by performing successive iterations, the optimal TAC is determined.

3.2. Partial Heat Integration PSD

This configuration is created by applying changes to the conventional arrangement. There are two possible ways to create this arrangement. If $Q_{CON}^{HPC} > Q_{REB}^{LPC}$ the LPC reboiler is eliminated and a side condenser added. If$Q_{CON}^{HPC} < Q_{REB}^{LPC}$the condenser of the HPC is removed and a side reboiler added. In the current condition, as shown in Fig. 3 A, the condenser of the HPC is removed. A heat exchanger between two

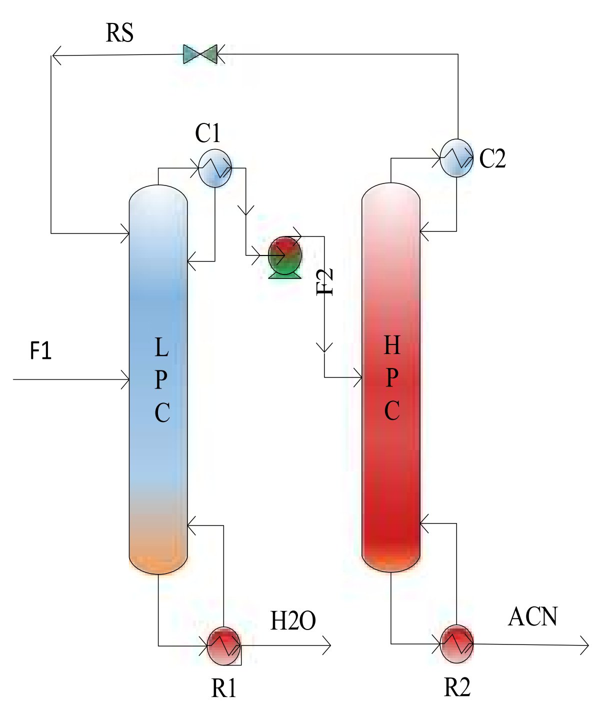

Fig. 2. : Conventional PSD (1).

Table 3
Optimization variable limit.

Optimization Variable	Lower bound	Upper bound
LPC tray number	5	75
HPC tray number	5	75
LPC inlet tray	1	75
HPC inlet tray	1	75
Recycle stream inlet tray	1	75
HPC pressure(bar)	1.1	10
HPC reflux ratio	0.05	12
LPC reflux ratio	0.05	12
Recycle stream flowrate(kg mole/hr)	1	600

columns with Q_{CON}^{HPC}power provides the total reflux rate required for HPC and a portion of the boil-up rate needed in the LPC. The side reboiler supplies the remainder of the boil-up rate.

3.3. Full Heat Integration PSD

Fig. 3 B illustrates the workings of this arrangement. The steam flow from the top of the HPC directly enters a heat exchanger and loses heat. The liquid flow from the LPC also enters this heat exchanger and turns into steam. In this arrangement, the condenser of the HPC supplies the entire heat required to provide the boil-up rate of the LPC, and there is no need to use a side condenser or a side reboiler. During optimization, the process variables are adjusted so that $Q_{CON}^{HPC} = Q_{REB}^{LPC}$.

3.4. Conventional PSD-Heat pump

Using the heat pump concept can significantly reduce energy consumption in the PSD process. To implement this idea, the exit steam from the top of the columns enters a compressor and its temperature increases as the pressure increases. This increase in temperature should be enough to provide the boil-up rate of the column. This concept can be applied to both LPC and HPC simultaneously. In a distillation column, the temperature of the lower part of the tower is higher than that of the upper part. Fig. 4 A and B illustrate the application of the heat pump concept to the HPC & the LPC respectively. In Fig. 4 C, this idea is used simultaneously in both columns.

3.5. External HIDiC-PSD

Another method for using thermal driving force in the PSD process is external heat integration. In this method, part (and not all) of the steam exiting from the HPC enters a heat exchanger and transfers heat with the LPC bottom liquid. Unlike the complete thermal integration method, it is possible to use a heat pump. The best location to place the external heat exchanger is determined based on the maximum amount of thermal driving force. There is the most significant temperature difference between the first tray of the HPC and the last tray in the LPC. The basic arrangement of external thermal integration is shown in Fig. 5 A. Functionally; this arrangement is similar to the FHI. The main difference is that, unlike FHI, it is possible to use a heat pump in this arrangement. The heat pump idea for the HPC is shown in Fig. 5B. Fig. 5C shows the result of implementing the heat pump idea in LPC and external thermal integration. In Fig. 5D, the heat pump concept is used in both towers simultaneously.

3.6. Two Concentric Columns -IHIDiC-PSD

Using the IHIDiC idea is a favorable option to reduce PSD costs. The possibility of using this concept in the form of two concentric columns or a DWC is there to do the PSD process. If the approach based on two concentric columns is chosen, the middle column will be of high pressure as in this way, it will be less costly to increase the thickness. One crucial point should be noted if using these methods based on internal heat integration for the PSD process. Due to the high-temperature difference between the two columns, if the heat transfer is done directly, the liquid in LPC will vaporize, and virtually no mass transfer will occur. As a measure against this, the outer wall of the HPC is covered by suitable insulation (polyester). The insulation's thickness and surface are set, so that the heat transfer process is carried out correctly. Fig. 6A displays the typical configuration of the IHIDiC-Two concentric column. In this case, the heat transfer is adjusted so that the heat exchange provides the reflux rate of the HPC.

In this case, using the heat pump idea on the towers is possible both separately or simultaneously. Heat pumps may be applied to HPC in Fig. 6B and to LPC in Fig. 6C. An essential point in HPC VRC is to use a reboiler next to the existing converter (after the compressor). The reason for this is related to the analysis of the coefficient of performance of heat pumps. Under normal conditions, the performance coefficient of the heat pump is 1.72, which indicates the ineffectiveness of this idea for this arrangement. Also, to remove the reboiler, the compression ratio in the compressor should reach 235, which leaves no economic justification. To resolve this issue, the heat pump and side reboiler may be used simultaneously. In Fig. 6D, the heat pump idea is applied to both towers.

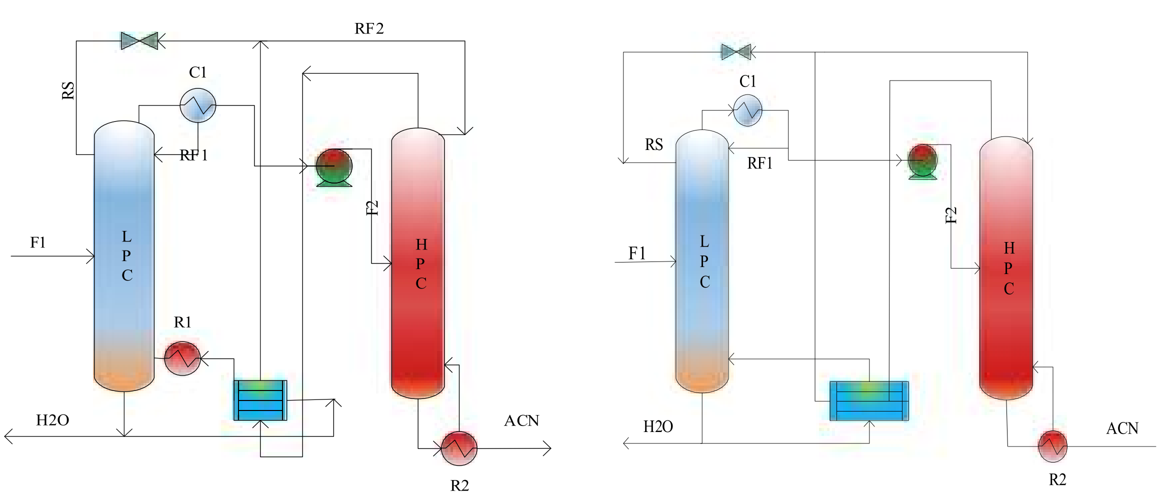

A: Partial heat integration PSD (2) **B**: Full heat integration PSD (3)

Fig. 3. Partial and full heat integration for the PSD process.

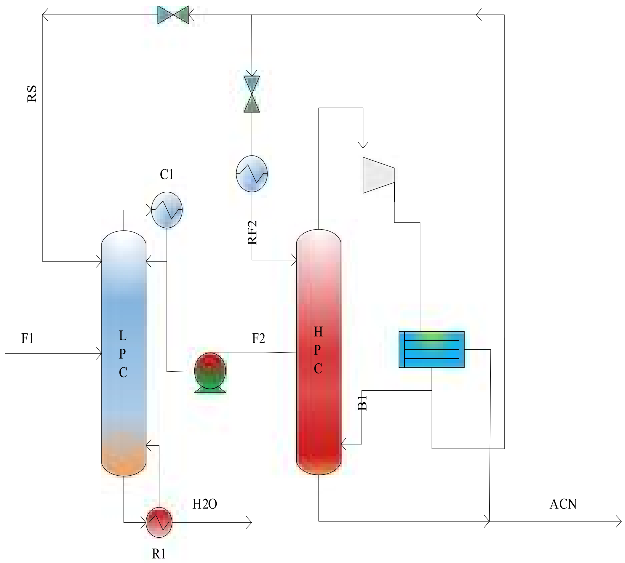

A: Conventional PSD-HPC VRC (4)

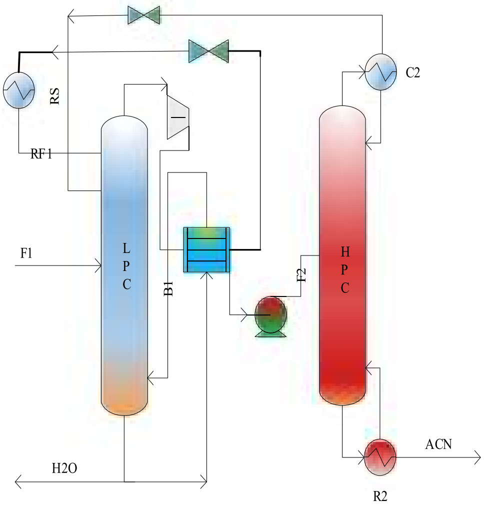

B: Conventional PSD-LPC VRC (5)

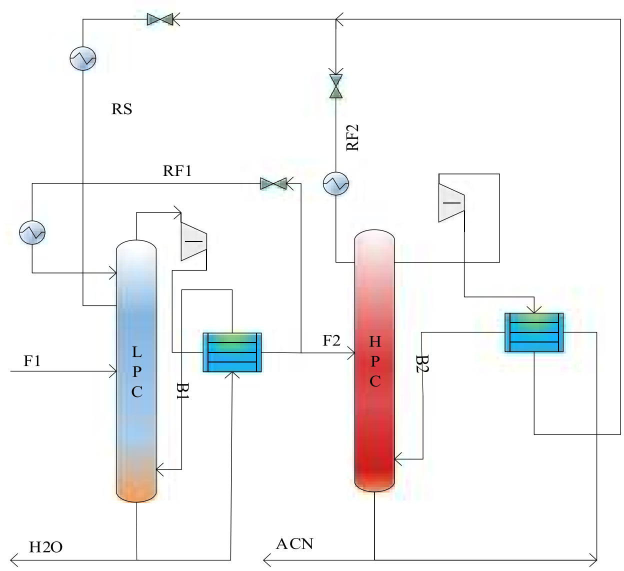

C: Conventional PSD-Two VRC (6)

Fig. 4. : Three configurations resulting from applying the VRC idea to the conventional PSD arrangement.

3.7. Divided Wall Column- Internal HIDiC-PSD

The second method to benefit from the concept of internal thermal integration is to use a tower and a partition wall between the columns. This wall transfers heat from the HPC to the LPC. It should be noted that in this method, wall insulation is used to prevent the evaporation of the entire liquid in the LPC. Heat transfer rate can increase the thickness of the wall, but this will cost more than insulating. The idea of the heat pump is also used here, and the three different arrangements that can be obtained along with the main configuration are shown in Fig. 7.

4. Results

During this study, four basic layouts are optimized, the results being presented in Table 4. Layouts 1, 3, 11, and 15 are basic configurations. Arrangements 2, 4–10 are taken from arrangement 1, and arrangements 12–14 from configuration 11. Configuration 15 is also considered the base for layouts 15–18. Other important information about the layouts, such as the power of reboilers, condensers, compressors, etc., is provided in Table 5.

Economic analysis of processes includes investment and annual operating costs. Fig. 8 evaluates the performance of different sequences based on investment costs. The results show that the lowest investment cost is related to the 3rd arrangement, which equals 1.03 M$/year. This arrangement has reduced the investment cost by 24.81% compared to the conventional configuration (1). This has several reasons. The first factor is the lack of compressors (expensive equipment) in this process. The second point is removing the reboiler and condenser and replacing them with a heat exchanger. According to the results, using the VRC idea has led to an increase in investment costs due to the presence of the compressor. The second place belongs to the 17th arrangement with a value of 1.19 M$/year. The configuration with the highest capital cost was 10, which shows an increase of 227% compared to the conventional configuration (1).

The evaluation results of different layouts in terms of operating costs are shown in Fig. 9. The first rank of the lowest operational cost value belongs to the 10th layout which is equal to 0.07 M$/year, showing a 92.5% reduction compared to the 1st layout. In this arrangement, the

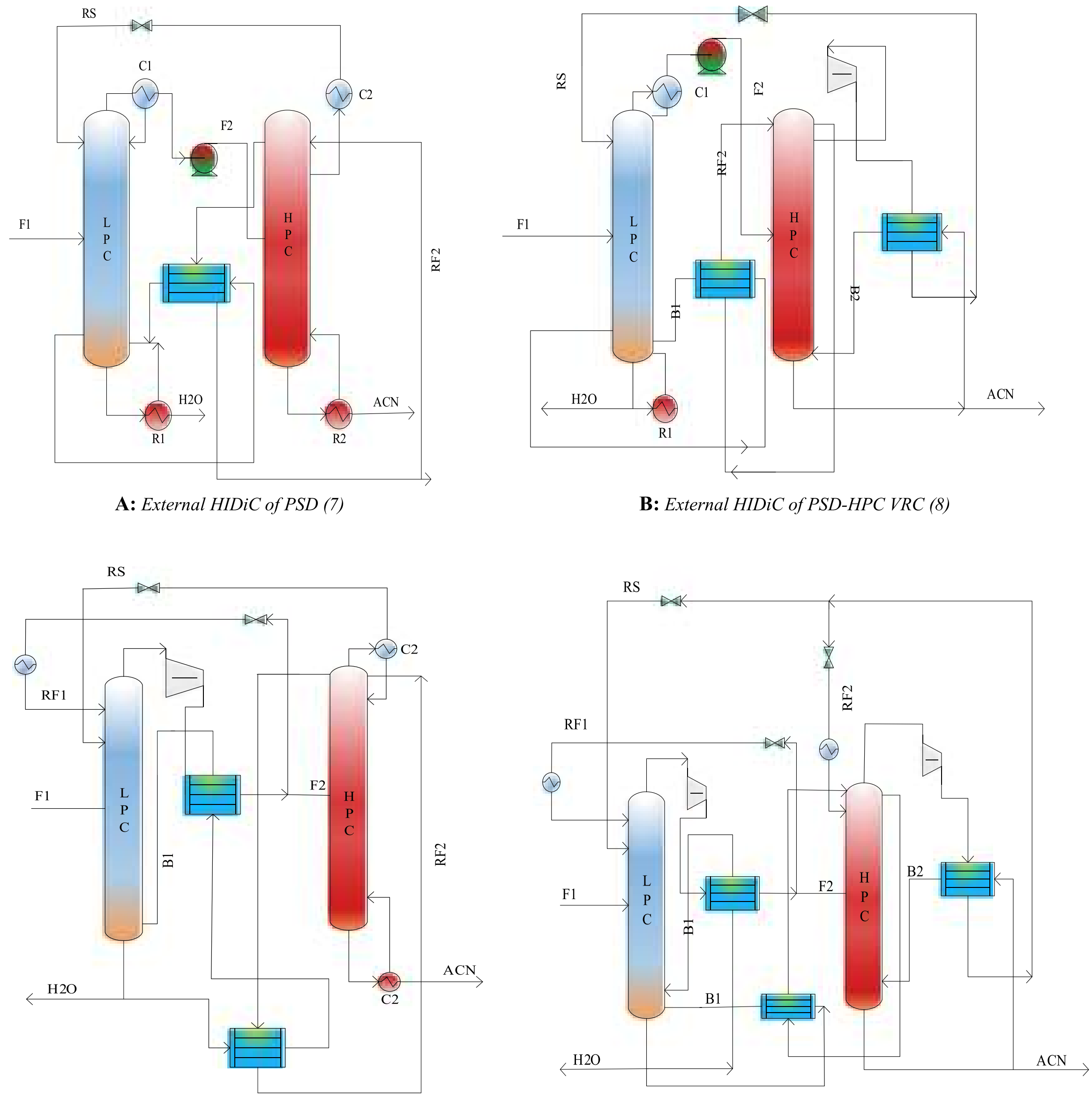

A: *External HIDiC of PSD (7)*

B: *External HIDiC of PSD-HPC VRC (8)*

C: *External HIDiC of PSD-LPC VRC (9)*

D: *External HIDiC of PSD-Two VRC (10)*

Fig. 5. : Four External HIDiC configurations.

idea of VRC is used in both columns. The use of this technique leads to the elimination of costs related to the steam used in the reboiler and the cooling water used in the condenser. In general, the use of VRC leads to the reduction of operating costs. On the other hand, according to the obtained results, the use of the HIDiC technique also leads to the reduction of operating costs, which is due to the reduction of steam consumption in the reboiler and cooling water in the condenser. In the 2nd place is the 18th layout, with a value of 0.087 M$/year. All arrangements are more economical than the 1st in terms of operating costs.

For different layouts, TAC results are shown in Fig. 10. The 18th arrangement with 0.388 M$/year is the least expensive. This configuration ranks 9th in terms of investment costs and 2nd place in terms of operational costs. This configuration reduces the TAC index by 299 percent compared to the 1st configuration. The 3rd layout has the lowest investment cost and ranks fourth in the TAC index. The 10th arrangement has the lowest operating cost, but it is in the second place from the point of view of the TAC index. All layouts have less TAC than the 1st.

The CO_2 emission index was used as a measure of environmental friendliness. The results of these evaluations are shown in Fig. 11. The 18th arrangement has the lowest CO_2 emission with an emission rate of 196 Ton CO_2/year. The second rank belongs to the 6th arrangement. The 10th layout is also in third place in terms of CO_2 emissions. These three layouts reduce carbon dioxide emissions by 96.33, 90.7, and 87.5%, respectively. It is quite clear that the use of VRC and HIDiC techniques lead to the reduction of carbon dioxide emissions. The reason for this fact is the reduction of steam consumption in reboilers. Also, the layouts that use the VRC idea in both columns have a very high potential in terms of the environment as steam is not consumed in any of the two columns. Arrangements 18, 14, 10, and 6 that use VRC in both columns have the best performance from an environmental point of view.

Another index that was evaluated to compare the arrangements was η. The results of this evaluation are demonstrated in Fig. 12. The highest η is associated with arrangement 18, and its value is 20.78%. The second place belongs to layout 16 with a value of 11.22% and the third place to layout 6 with 10.78%. Using arrangements 8 and 11 leads to a decrease in η compared to arrangement 1. The thermodynamic efficiency of distillation towers is low. As it is known, in the best arrangement, this number reaches 20.78%. The use of exergy analysis to locate points losses mostly occur and remedy them can significantly increase the

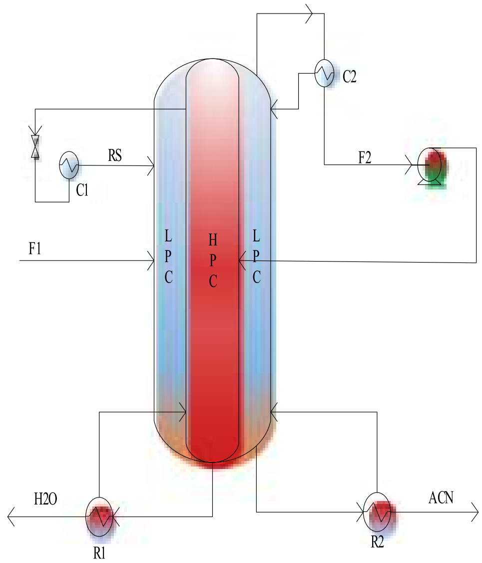

A: Internal HIDiC -Two Concentric Columns-PSD (11)

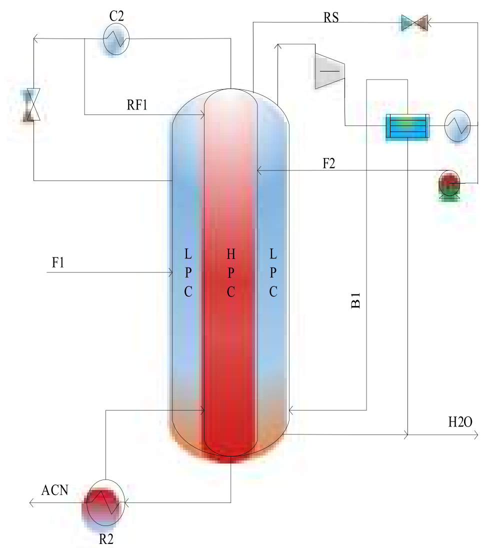

B: Internal HIDiC -Two Concentric Column -LPC VRC-PSD (12)

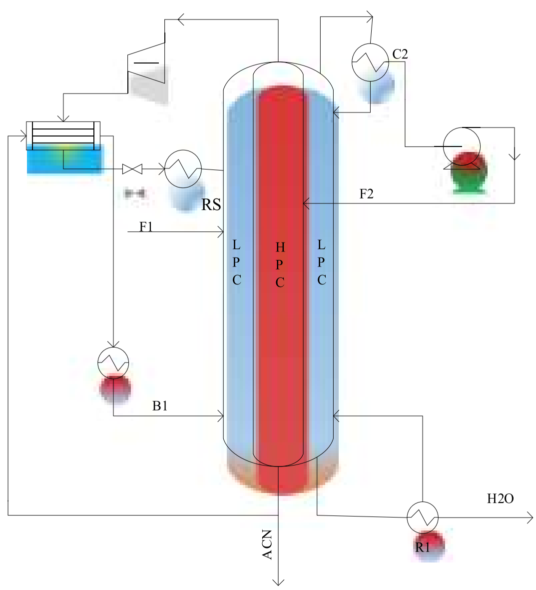

C: Internal HIDiC -Two Concentric Column -HPC VRC-PSD (13)

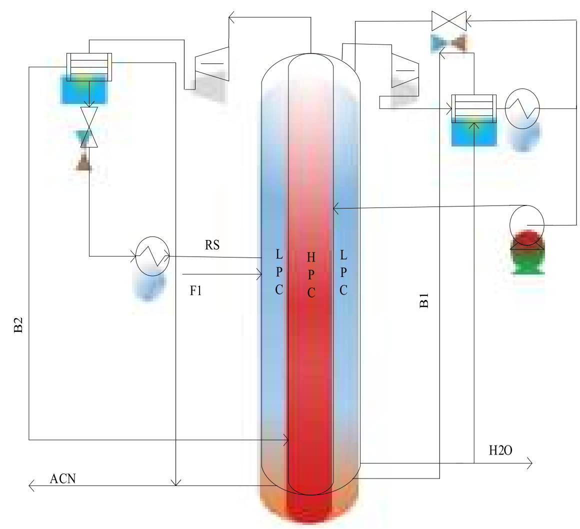

D: Internal HIDiC -Two Concentric Columns -Two VRC-PSD (14)

Fig. 6. : Four concentric HIDiC configurations.

thermodynamic efficiency of the distillation tower. In general, the use of VRC and HIDiC techniques does not have a great effect on the thermodynamic efficiency of the distillation tower (except in special cases such as 18 or 16 and 6 arrangement).

The results of checking the performance coefficient of heat pumps are shown in *Table 6* . This idea has been used in 12 different layouts. In 4 layouts, this idea is used dually. Arrangement 8 is the worst case regarding the heat pump performance index, with arrangement 5 having the most potential for applying the idea.

By checking the analysis done, it is clear that the 18th arrangement is the best among the presented configurations from the point of view of investment cost, this arrangement has a cost of 1.85 million dollars (M $), with a 35% increase compared to the conventional layout. This layout has the lowest investment cost among the dual layouts. The reason for this is the use of relatively small compressors (37 and 93 kW) and the use of one shell. From the point of view of operating costs, this arrangement has shown a very high potential by removing the reboiler and condenser of both towers, and with a reduction of 90.69%, this number has reached a very low value of 0.087% and stands at the second place only to the 10th arrangement. From the point of view of the TAC index, this arrangement has brought this number to 0.388 *M$/Year* with a decrease of 66.55% compared to the conventional configuration. Due to the elimination of fuel consumption of reboilers, this arrangement has also performed very well from an environmental point of view and has brought this amount to 197 tons per year with a 96.31% reduction.

5. Discussions

Based on the results of this investigation, the use of FHI and PHI configurations will lead to a decrease in operating costs. The reason is the reduction of steam consumption in PHI and the elimination of steam consumption in FHI. According to the results in Fig. 9, it is clear that the FHI and PHI arrangements have a lower operating costs than the conventional arrangement. Reduction of operating costs due to decreasing steam consumption will also lead to the reduction of carbon dioxide emissions. According to the results obtained in η section, reducing energy consumption has led to an increase in η. Based on the results, PHI investment cost is lower than that in the conventional configurations.

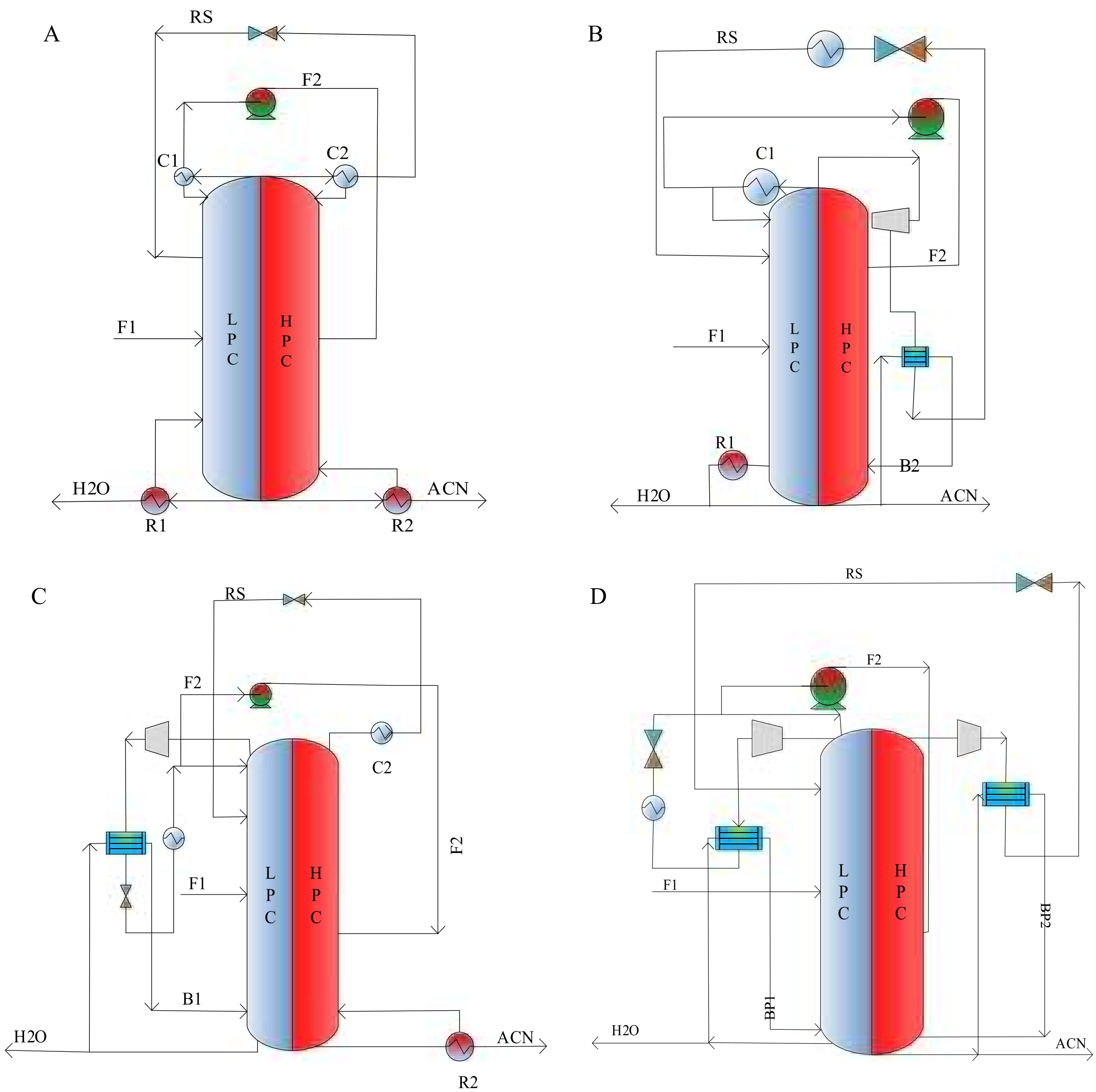

Fig. 7. **:** Schematic demonstration of configurations 15–18;**(A)** Internal HIDiC -Divided Wall Column-PSD (15);**(B)** Internal HIDiC -Divided Wall Column-HPC VRC-PSD (16);**(C)** Internal HIDiC -Divided Wall Column-LPC VRC-PSD (17);**(D)** Internal HIDiC -Divided Wall Column-Two VRC-PSD (18).

Table 4
Optimization results.

Configurations Variables	Conventional	Full heat integrations	Internal HIDiC-Concentric column	Internal HIDiC-Divided wall column
LPC reflux ratio	0.15	0.15	0.23	0.26
HPC reflux ratio	0.24	0.65	0.87	0.43
LPC tray number	17	13	18	19
HPC tray number	16	13	18	19
LPC feed input tray	11	10	14	15
HPC feed input tray	8	7	7	11
Recycle input tray	11	8	14	17
HPC pressure (bar)	9.63	7.15	7.20	9.05
Recycle stream flowrate (kmole/hr)	61.58	67.48	61.96	55.02

The reason is the elimination of one heat exchanger (condenser or reboiler) and the reduction in the area of the other exchanger. In contrast, a definitive assessment of the investment costs under FHI remains challenging. Despite the removal of both reboiler and condenser costs, the altered operating conditions introduce uncertainties, preventing a conclusive judgment on its economic viability.

The evaluation of combining the arrangements resulting from the use of VRC on the conventional arrangement determined that the amount of energy consumption in these arrangements has been reduced. The reason for this is the removal of reboiler and condenser (source of energy consumption). Reducing the amount of steam consumption will also lead to the reduction of carbon dioxide emissions. According to the results of the investment cost evaluation, the arrangements that used the VRC technique have a higher investment cost, which is due to the presence of the compressor. Therefore, the VRC technique will lead to an increase in investment costs, a decrease in operating costs, a decrease in carbon dioxide emissions, and an increase in thermodynamic efficiency. However, economic viability is contingent on factors such as compressor cost, fuel prices, and fuel rate savings, all of which vary based on the specific case study and its characteristics.

The use of EHIDiC leads to a reduction in the amount of steam

Table 5
Detailed information on Configurations.

Config	Q_{LPC}^{REB} (KW)	Q_{HPC}^{REB} (KW)	Q_{LPC}^{CON} (KW)	Q_{HPC}^{CON} (KW)	Q_{LPC}^{COMP} (KW)	Q_{HPC}^{COMP} (KW)	OPERATING COST (M $/Year)	Capital Cost (M $)	Q of side reboilers (KW)	Q of side condensers (KW)	Total energy consumption (KW) (QR+3QC) (Xia et al., 2017)
1	959	876	-954	-669	0	0	0.935	1.37	0	0	1835
2	291	877	-954	0	0	0	0.604	1.31	291	0	1459
3	0	1185	-1021	0	0	0	0.581	1.03	0	0	1185
4	903	0	-955	0	0	278	0.616	2.15	0	-14.4	1737
5	0	808	0	-665	110	0	0.492	2.16	0	-39.2	1138
6	0	0	0	0	110	218	0.200	2.75	0	-100.6	984
7	830	877	-955	-539	0	0	0.871	1.36	0	0	1707
8	782	0	-955	0	0	385	0.623	2.53	0	0	1937
9	0	877	0	-605	111	0	0.529	2.79	0	-171.0	1210
10	0	0	0	0	111	322	0.070	3.12	0	-220.5	1299
11	497	1208	-1023	-482	0	0	0.878	1.38	0	0	1705
12	0	1213	0	-555	101	0	0.657	1.98	0	-449.0	1516
13	563	0	-1023	0	0	129	0.650	1.99	573	-49.3	1523
14	0	0	0	0	101	129	0.414	2.43	573	-497.5	1263
15	499	881	-958	-484	0	0	0.845	1.26	0	0	1380
16	774	0	-961	0	0	37	0.714	1.29	0	-328.3	885
17	0	883	0	-555	93	0	0.521	1.19	0	-369.8	1162
18	0	0	0	0	93	37	0.087	1.85	0	-702.3	390

consumed, which will reduce operating costs. From the point of view of investment costs, the use of a compressor and heat exchanger network leads to an increase in investment costs, and on the other hand, reducing the area of reboiler and condenser leads to a decrease in investment costs. But in general, according to the existing results, it may be said that these arrangements will have a higher investment cost due to the use of a compressor. According to the available environmental results, EHIDiC is an environmentally friendly process that emits less carbon dioxide than the conventional configuration. The evaluation of using the idea of IHIDiC is similar to EHIDiC. With the difference that the construction of IHIDiC-based systems is more difficult, which will lead to a further reduction in operating costs. These systems consume less energy and emit less carbon dioxide. Using a compressor leads to an increase in the investment costs and removing one of the columns leads to a decrease in it. This is completely dependent on the condition and nature of feed and various other factors.

The adoption of the divided (splitting) wall column is a novel technique explored in limited studies. This approach, particularly effective when the temperature difference between the two parts is maximal, exhibits a promising potential. In terms of investment cost, these arrangements have led to a decrease in this index by making the reboiler and condenser smaller and also using one column. On the other hand, the use of a compressor has also led to an increase in investment costs. However, the use of these arrangements will definitely reduce the operating costs and the emission of carbon dioxide will also be reduced. Further in-depth investigations, including safety and controllability analyses, are essential to unveil the strengths and weaknesses of this arrangement.

It is crucial to acknowledge that economic evaluations are contingent on equipment and fuel prices, as well as variations in loan interest rates and repayment periods across different countries. The economic comparison between layouts is, therefore, inherently tied to the specific application context and prevailing prices in the corresponding geographical area.

6. Conclusions

In this comprehensive study, we conducted a comparative analysis of various PSD configurations, presenting innovative results that redefine the landscape of this process. The integration of internal and external thermal concepts, coupled with the revolutionary heat pump idea, has given rise to novel PSD arrangements. The incorporation of the heat pump eliminates the need for a reboiler, resulting in a substantial reduction in fossil fuel consumption and an impressive decrease in CO_2 emissions across all sequences. The utilization of these novel ideas and concept combinations translates directly into a noteworthy reduction in annual costs.

From an economic standpoint, the most optimal arrangement emerges as configuration 18, utilizing simultaneous internal thermal integration of the middle wall and the heat pump, boasting a TAC of 0.388 M$/year. This represents a remarkable 66.5% reduction compared to configuration 1. Addressing a global concern, configuration 18 significantly reduces carbon dioxide emissions by an impressive 96%, bringing the total to a mere 197 tons per year. Furthermore, this configuration exhibits superior η, reaching a value of 20.78%.

While these economic and environmental indicators provide crucial insights, a comprehensive decision regarding the optimal layout should also consider process safety and controllability. As we move forward, exploration of alternative azeotropic separation methods, such as extractive distillation, azeotropic distillation, and membrane processes are also plausible. The selection of the ultimate best structure for industrialization demands a meticulous assessment of each method's optimal configuration. Only through this thorough evaluation can one confidently recommend and implement the most efficient and environmentally sustainable PSD arrangement for industrial applications.

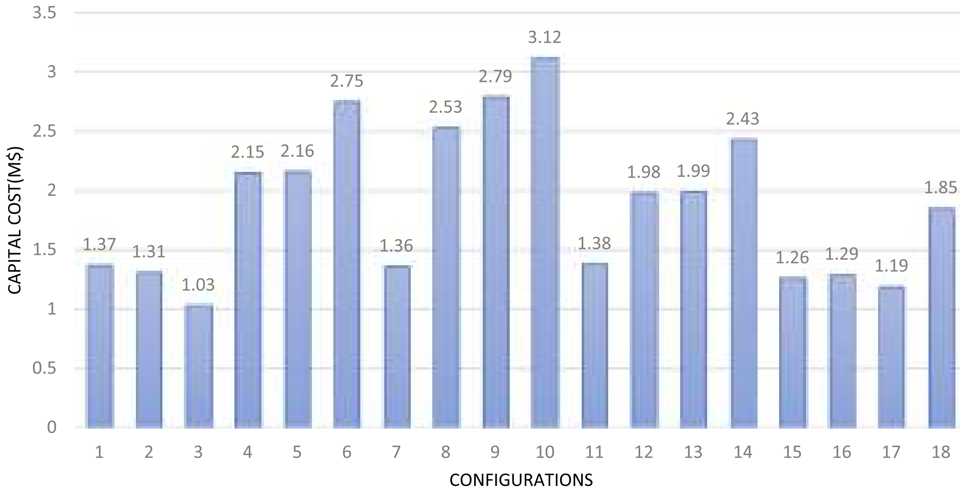

Fig. 8. : Capital costs of PSD configurations.

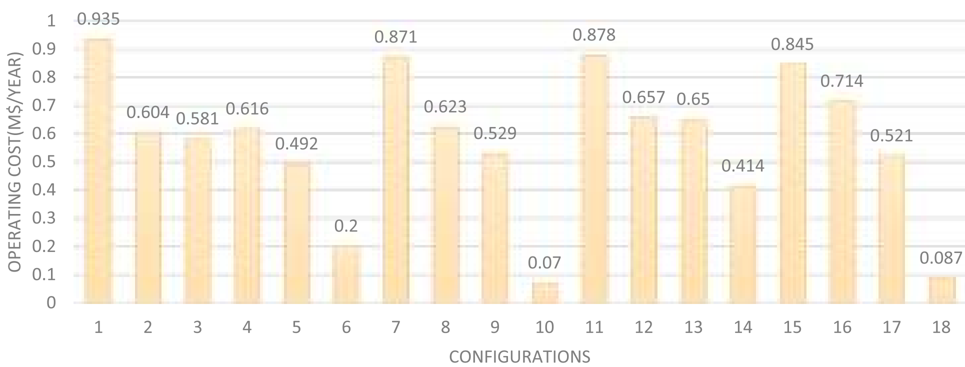

Fig. 9. : Operating costs of PSD configurations.

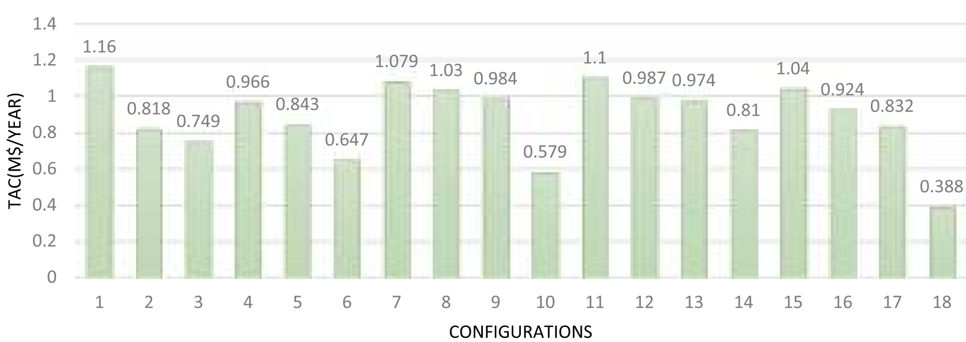

Fig. 10. : TAC of PSD configurations.

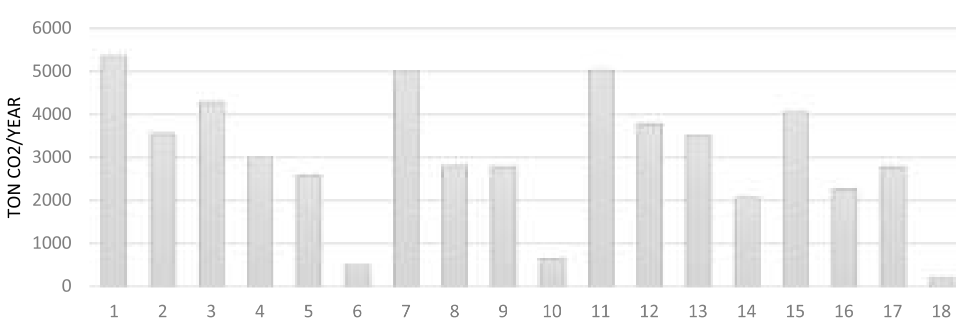

Fig. 11. : CO_2 emissions of PSD configurations.

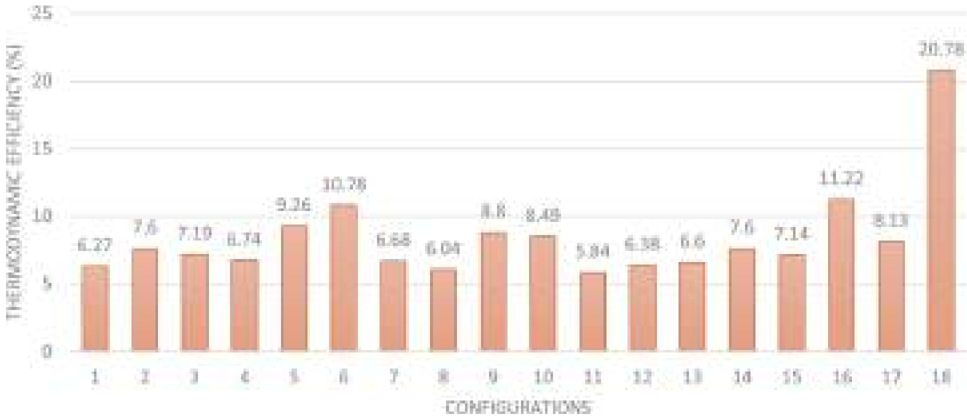

Fig. 12. **:** Thermodynamic efficiencies (%) of PSD configurations.

Table 6
The results of the analysis of the configurations.

Configuration	*TAC (M$/Year)*	*TAC save%*	*Coefficient of performance (COP)*		*Thermodynamic efficiency (%)*	*CO2 emission (Ton/Year)*
1	1.160	0	-		6.27	5352
2	0.818	29.50	-		7.60	3543
3	0.749	35.47	-		7.19	4280
4	0.966	16.75	3.71		6.74	2989
5	0.843	27.36	8.8		9.26	2582
6	0.647	44.26	LPC	8.8	10.78	495
			HPC	3.71		
7	1.079	5.75	-		6.68	4983
8	1.030	10.80	2.71		6.04	2807
9	0.984	15.18	7.5		8.80	2790
10	0.579	50.07	LPC	7.5	8.49	655
			HPC	2.71		
11	1.100	5.16	-		5.84	5029
12	0.987	15.64	4.93		6.38	3780
13	0.974	16.03	4.77		6.60	3509
14	0.810	30.19	LPC	4.77	7.60	2061
			HPC	4.93		
15	1.040	9.49	-		7.14	4056
16	0.924	20.34	5.72		11.22	2260
17	0.832	28.27	5.17		8.13	2784
18	0.388	66.55	LPC	5.17	20.78	197
			HPC	5.72		

Declaration of Competing Interest

The authors declare that they have no known competing financial interests or personal relationships that could have appeared to influence the work reported in this paper.

Appendix A

Table A.1
Equipment Cost

Equipment		**Cost**	
Column vessel		$\left(\frac{M\&S}{280}\right)\cdot 937.636\cdot D^{1.066}\cdot H^{.802}\cdot(2.18+Fc)$	
D: Diameter of column (m)			
H: Length of column (m)			
Fc=Fm *Fp			
Fm =3.67 (Shell material)			
Fp can be obtained from the following table			
Pressure(atm)	≥3.4	6.8	13.6
Fp	1.00	1.05	1.15
Column Tray		$\left(\frac{M\&S}{280}\right)\cdot 97.243\cdot D^{1.55}\cdot H.Fc$	
Fc=Fs+Ft+Fm			
Fs=1(Tray space), Ft=0(Tray type), Fm=1.17(Tray material)			
Heat Exchanger		$\left(\frac{M\&S}{280}\right)\cdot 474.668.A^{.65}\cdot(2.29+Fc)$	
Fc=(Fd+Fp). Fm			
Fm=3.75(Shell and tube material)			

(*continued on next page*)

Table A.1 (*continued*)

Equipment			Cost	
Fd=1.35(kettle reboiler),0.8(fixed tube sheet heat exchanger)				
Fp can obtain the following table				
Pressure(atm)		≥10.2	20.4	27.2
54.4				
Fp	0.00	0.10	0.25	0.52
Compressor			$\left(\frac{M\&S}{280}\right) \cdot 517.5 \cdot bhp^{0.85} \cdot (2.11 + Fc)$	
Fc=1(Compressor type)				
Insulation cost:$15\frac{\$}{m2}$				

Table A.2
Operating Cost

Type	Cost
LP steam(433 K)	**13.28 $/GJ**
MP steam(457 K)	**14.9 $/GJ**
HP steam(537 K)	**17.7 $/GJ**
Cooling water	**.354 $/GJ0**
Electrical cost	**.06 $/kwh0**
Here M&S=1431.7	

Appendix A. Supporting information

Supplementary data associated with this article can be found in the online version at doi:10.1016/j.cherd.2024.02.033.

References

Huang, H.-J., Ramaswamy, S., Tschirner, U., Ramarao, B., 2010. Separation and Purification processes for lignocellulose-to-bioalcohol production. in: Bioalcohol production. Elsevier, pp. 246–277.

Lü, L., Zhu, L., Liu, H., Li, H., Sun, S., 2018. Comparison of continuous homogenous azeotropic and pressure-swing distillation for a minimum azeotropic system ethyl acetate/n-hexane separation. Chin. J. Chem. Eng. 26, 2023–2033.

Xu, Q., Wang, Z., Dai, Y., Zhao, Q., Li, Y., Cui, P., Zhu, Z., Wang, Y., Gao, J., Ma, Y., 2022. Economy, Exergy, energy consumption and environmental human toxicity potential assessment of vacuum extractive distillation coupled pervaporation process for separating Acetone/Isopropanol/Water Multi-azeotropes system. Sep. Purif. Technol. 300, 121834.

Zhang, H., Wang, S., Tang, J., Li, N., Li, Y., Cui, P., Wang, Y., Zheng, S., Zhu, Z., Ma, Y., 2021. Multi-objective optimization and control strategy for extractive distillation with dividing-wall column/pervaporation for separation of ternary azeotropes based on mechanism analysis. Energy 229, 120774.

Li, X., Ye, Q., Li, J., Yan, L., Jian, X., Xie, L., Zhang, J., 2022. Investigation of energy-efficient heat pump assisted heterogeneous azeotropic distillation for separating of acetonitrile/ethyl acetate/n-hexane mixture. Chin. J. Chem. Eng.

Qi, J., Li, Y., Xue, J., Qiao, R., Zhang, Z., Li, Q., 2020. Comparison of heterogeneous azeotropic distillation and energy-saving extractive distillation for separating the acetonitrile-water mixtures. Sep. Purif. Technol. 238, 116487.

Zhu, J., Hao, L., Wei, H., 2021. Sustainable concept design including economic, environment and inherent safety criteria: process intensification-reactive pressure swing distillation. J. Clean. Prod. 314, 127852.

Shi, P., Zhang, Q., Zeng, A., Ma, Y., Yuan, X., 2020. Eco-efficient vapor recompression-assisted pressure-swing distillation process for the separation of a maximum-boiling azeotrope. Energy 196, 117095.

Zhang, Q., Yang, S., Shi, P., Hou, W., Zeng, A., Ma, Y., Yuan, X., 2020. Economically and thermodynamically efficient heat pump-assisted side-stream pressure-swing distillation arrangement for separating a maximum-boiling azeotrope. Appl. Therm. Eng. 173, 115228.

Ferchichi, M., Hegely, L., Lang, P., 2022. Economic and environmental evaluation of heat pump-assisted pressure-swing distillation of maximum-boiling azeotropic mixture water-ethylenediamine. Energy 239, 122608.

Xia, H., Ye, Q., Feng, S., Li, R., Suo, X., 2017. A novel energy-saving pressure swing distillation process based on self-heat recuperation technology. Energy 141, 770–781.

Wang, K., Li, J., Liu, P., Lian, M., Du, T., 2019. Pressure swing distillation for the separation of methyl acetate-methanol azeotrope. Asia-Pac. J. Chem. Eng. 14, e2319.

Wang, Y., Zhang, Z., Xu, D., Liu, W., Zhu, Z., 2016. Design and control of pressure-swing distillation for azeotropes with different types of boiling behavior at different pressures. J. Process Control 42, 59–76.

Li, J., Wang, K., Lian, M., Li, Z., Du, T., 2019a. Process simulation of the separation of aqueous acetonitrile solution by pressure swing distillation. Processes 7, 409.

Zhu, Z., Wang, L., Ma, Y., Wang, W., Wang, Y., 2015. Separating an azeotropic mixture of toluene and ethanol via heat integration pressure swing distillation. Comput. Chem. Eng. 76, 137–149.

Liang, S., Cao, Y., Liu, X., Li, X., Zhao, Y., Wang, Y., Wang, Y., 2017. Insight into pressure-swing distillation from azeotropic phenomenon to dynamic control. Chem. Eng. Res. Des. 117, 318–335.

McConvey, I.F., Woods, D., Lewis, M., Gan, Q., Nancarrow, P., 2012. The importance of acetonitrile in the pharmaceutical industry and opportunities for its recovery from waste. Org. Process Res. Dev. 16, 612–624.

Zhang, D., Zhang, Y., Wen, Y., Hou, K., Zhao, J., 2011. Intrinsic kinetics for the synthesis of acetonitrile from ethanol and ammonia over Co–Ni/γ–Al2O3 catalyst. Chem. Eng. Res. Des. 89, 2147–2152.

Sazonova, A.Y., Raeva, V.M., 2015. Recovery of acetonitrile from aqueous solutions by extractive distillation–Effect of entrainer. Int. J. Chem. Mol. Nucl. Mater. Metall. Eng. 9, 288–291.

Rezaie, F., Pirouzfar, V., Alihosseini, A., 2020. Technical and economic analysis of acrylonitrile production from polypropylene. Therm. Sci. Eng. Prog. 16, 100463.

Kiss, A.A., Smith, R., 2020. Rethinking energy use in distillation processes for a more sustainable chemical industry. Energy 203, 117788.

Dejanović, I., Matijašević, L., Olujić, Ž., 2010. Dividing wall column—A breakthrough towards sustainable distilling. Chem. Eng. Process.: Process.Intensif. 49, 559–580.

Kazemi, A., Rasti, Y., Mehrabani-Zeinabad, A., Beheshti, M., 2018. Evaluation of a novel configuration of bottom flashing on dual distillation columns for saving energy. Int. J. Ind. Chem. 9, 75–84.

Huang, K., Shan, L., Zhu, Q., Qian, J., 2008. Adding rectifying/stripping section type heat integration to a pressure-swing distillation (PSD) process. Appl. Therm. Eng. 28, 923–932.

Shan, B., Sun, D., Zheng, Q., Zhang, F., Wang, Y., Zhu, Z., 2021. Dynamic control of the pressure-swing distillation process for THF/ethanol/water separation with and without thermal integration. Sep. Purif. Technol. 268, 118686.

You, X., Ma, T., Qiu, T., 2019. Design and optimization of sustainable pressure swing distillation for minimum-boiling azeotrope separation. Ind. Eng. Chem. Res. 58, 21659–21670.

Luyben, W.L., 2018. Design and control of a pressure-swing distillation process with vapor recompression. Chem. Eng. Process. -Process. Intensif. 123, 174–184.

Li, X., Geng, X., Cui, P., Yang, J., Zhu, Z., Wang, Y., Xu, D., 2019b. Thermodynamic efficiency enhancement of pressure-swing distillation process via heat integration and heat pump technology. Appl. Therm. Eng. 154, 519–529.

Maddu, S., Malik, R.K., 2011. A Design methodology for Internally HeatIntegrated Distillation Columns (IHIDiC) with side condensers and side reboilers (SCSR). In: in: Computer Aided Chemical Engineering, Vol. 29. Elsevier, pp. 412–416.

Gadalla, M., Olujic, Z., Esteller, L.J., Guillén-Gosálbez, G., 2007. A design method for internal heat integrated distillation columns (iHIDiCs). In: in: Computer Aided Chemical Engineering, Vol. 24. Elsevier, pp. 1041–1046.

Shahandeh, H., Jafari, M., Kasiri, N., Ivakpour, J., 2015. Economic optimization of heat pump-assisted distillation columns in methanol-water separation. Energy 80, 496–508.

Jana, A.K., 2010. Heat integrated distillation operation. Appl. Energy 87, 1477–1494.

Jana, A.K., 2016. A new divided-wall heat integrated distillation column (HIDiC) for batch processing: feasibility and analysis. Appl. Energy 172, 199–206.

Shahandeh, H., Ivakpour, J., Kasiri, N., 2014. Internal and external HIDiCs (heat-integrated distillation columns) optimization by genetic algorithm. Energy 64, 875–886.

Khalili, N., Kasiri, N., Ivakpour, J., Khalili-Garakani, A., Khanof, M., 2020. Optimal configuration of ternary distillation columns using heat integration with external heat exchangers. Energy 191, 116479.
Gadalla, M.A., 2009. Internal heat integrated distillation columns (iHIDiCs)—new systematic design methodology. Chem. Eng. Res. Des. 87, 1658–1666.
Suphanit, B., 2010. Design of internally heat-integrated distillation column (HIDiC): uniform heat transfer area versus uniform heat distribution. Energy 35, 1505–1514.
Kiss, A.A., Olujić, Ž., 2014. A review on process intensification in internally heat-integrated distillation columns. Chem. Eng. Process.: Process.Intensif. 86, 125–144.
Zhang, Z., Wang, Y., Zhang, M., Guang, C., Li, M., Gao, J., 2022. Energy-saving investigation of pressure-swing distillation strengthening configurations for benzene/isobutanol binary azeotrope. Sep. Purif. Technol. 296, 121381.
Zhai, J., Chen, X., Sun, X., Xie, H., 2023. Economically and thermodynamically efficient pressure-swing distillation with heat integration and heat pump techniques. Appl. Therm. Eng. 218, 119389.
Carlson, E.C., 1996. Don't gamble with physical properties for simulations. Chem. Eng. Prog. 92, 35–46.
You, X., Rodriguez-Donis, I., Gerbaud, V., 2016. Reducing process cost and CO2 emissions for extractive distillation by double-effect heat integration and mechanical heat pump. Appl. Energy 166, 128–140.
Wang, Y., Zhang, H., Yang, X., Shen, Y., Chen, Z., Cui, P., Wang, L., Meng, F., Ma, Y., Gao, J., 2020. Insight into separation of azeotrope in wastewater to achieve cleaner production by extractive distillation and pressure-swing distillation based on phase equilibrium. J. Clean. Prod. 276, 124213.
Mao, W., Cao, Y., Shen, R., Zhou, J., Zhou, X., Li, W., 2020. Heat integrated technology assisted pressure-swing distillation for the mixture of ethylene glycol and 1, 2-butanediol. Sep. Purif. Technol. 241, 116740.